Pck1 Gene Silencing in the Liver Improves Glycemia Control, Insulin Sensitivity, and Dyslipidemia in *db/db* Mice

Alicia G. Gómez-Valadés,[1] Andrés Méndez-Lucas,[1] Anna Vidal-Alabró,[1] Francese X. Blasco,[1] Miguel Chillon,[2] Ramon Bartrons,[1] Jordi Bermúdez,[1] and José C. Perales[1]

OBJECTIVE—Cytosolic phosphoenolpyruvate carboxykinase (PEPCK-C; encoded by *Pck1*) catalyzes the first committed step in gluconeogenesis. Extensive evidence demonstrates a direct correlation between PEPCK-C activity and glycemia control. Therefore, we aimed to evaluate the metabolic impact and their underlying mechanisms of knocking down hepatic PEPCK-C in a type 2 diabetic model.

RESEARCH DESIGN AND METHODS—PEPCK-C gene targeting was achieved using adenovirus-transduced RNAi. The study assessed several clinical symptoms of diabetes and insulin signaling in peripheral tissues, in addition to changes in gene expression, protein, and metabolites in the liver. Liver bioenergetics was also evaluated.

RESULTS—Treatment resulted in reduced PEPCK-C mRNA and protein. After treatment, improved glycemia and insulinemia, lower triglyceride, and higher total and HDL cholesterol were measured. Unsterified fatty acid accumulation was observed in the liver, in the absence of de novo lipogenesis. Despite hepatic lipidosis, treatment resulted in improved insulin signaling in the liver, muscle, and adipose tissue. O_2 consumption measurements in isolated hepatocytes demonstrated unaltered mitochondrial function and a consequent increased cellular energy charge. Key regulatory factors (FOXO1, hepatocyte nuclear factor-4α, and peroxisome proliferator–activated receptor-γ coactivator [PGC]-1α) and enzymes (G6Pase) implicated in gluconeogenesis were downregulated after treatment. Finally, the levels of Sirt1, a redox-state sensor that modulates gluconeogenesis through PGC-1α, were diminished.

CONCLUSIONS—Our observations indicate that silencing PEPCK-C has direct impact on glycemia control and energy metabolism and provides new insights into the potential significance of the enzyme as a therapeutic target for the treatment of diabetes. *Diabetes* 57:2199–2210, 2008

The liver has a central role in maintaining glucose and energy homeostasis. Postabsorptive metabolism in hepatocytes ensures glucose synthesis via gluconeogenesis and glycogenolysis to maintain blood glucose levels. In diabetic patients, sustained rates of gluconeogenesis independent of nutrient status are responsible for increased hepatic glucose output (HGO) and, therefore, hyperglycemia (1,2).

Phosphoenolpyruvate carboxykinase (PEPCK) catalyzes the first committed step in gluconeogenesis. Gene transcription from the cytosolic form of PEPCK (PEPCK-C) is highly regulated by the glucagon/insulin axis. In diabetes, the lack of insulin (type 1 diabetes) or resistance to its action (type 2 diabetes) is responsible for an important upregulation of the enzyme, and this induction correlates with increased rates of gluconeogenesis in liver and kidney (3). Also, PEPCK gene modulation in the liver has resulted in remarkable effects on systemic glucose metabolism in mice. A twofold overexpression of PEPCK-C results in insulin resistance (4), whereas a sevenfold overexpression results in hyperglycemia (5). Moreover, studies by Burgess et al. (6) and She et al. (7,8) using a liver-specific PEPCK-C knockout mouse have shed light on the critical role of PEPCK-C in the integration of energy metabolism through a mechanism that implicates cataplerosis from mitochondria, as highlighted by hypoglycemia and lethality after ablation of PEPCK-C gene in mice (7–9). Furthermore, a polymorphism in the promoter for *Pck1* is associated with the development of type 2 diabetes (10), and dysregulation of gluconeogenesis has direct implications for glucose homeostasis in humans (2,11).

Despite all evidence, the validation of this enzyme as a target for liver-specific gene therapy or pharmacological intervention in diabetes has not been extensively investigated to date. Prior studies in streptozotocin-treated mice using RNAi-directed downregulation of PEPCK-C in the liver have shown a direct role for this enzyme in the regulation of glucose homeostasis in the absence of insulin (12). Here, we have focused on evaluating the indirect metabolic impact of knocking down hepatic PEPCK-C in a model of insulin resistance.

We show that partial silencing of hepatic PEPCK-C in *db/db* mice leads to improved glycemia control directly, through the coordinate inhibition of components of the gluconeogenic pathway in the liver, and indirectly, by improving insulinemia and peripheral sensitivity to the hormone. Our observations indicate that PEPCK-C plays a key role in the control of hepatic energy metabolism and
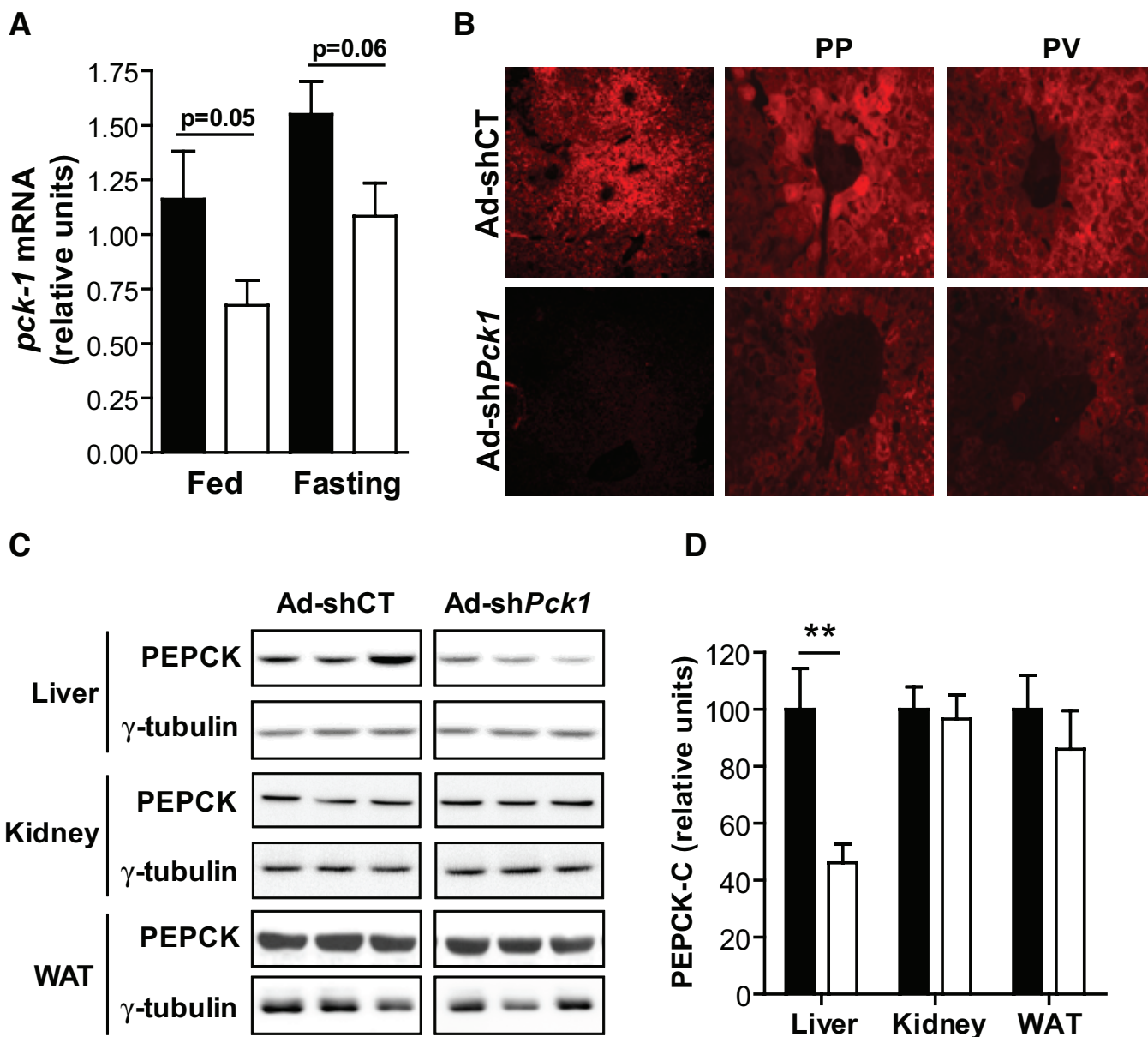
FIG. 1. Adenovirus-mediated shRNA knocks down PEPCK-C specifically in the liver. A dose of 6.67×10^{10} pfu/kg control (Ad-shCT) and PEPCK-C–directed shRNA (Ad-sh*Pck1*) adenovirus was injected in male, 6- to 8-week-old *db/db* mice. *A*: PEPCK-C expression analyzed by quantitative RT-PCR in fed ($n = 11$) or overnight-fasted ($n = 5$) animals 14 days after treatment. β-2-microglobulin was used as housekeeping gene. Data are represented as relative *Pck1* gene expression compared with control-fed animals (Ad-shCT). Data are means ± SE. Student's *t* test was used to discriminate statistical significance. *B*: PEPCK-C immunohistochemistry was performed in 7-μm cryosections obtained from livers treated with either control or PEPCK-C–targeted shRNA. Confocal microscopy was used to determine signal distribution throughout the liver acinus. ×100 (*right*) and ×400 image magnification blow up from periportal (PP) and perivenous (PV) zones are shown. Pictures are representative of three independent experiments. *C*: PEPCK-C immunodetection in total protein extracts from liver, kidney, and epididymal WAT. γ-Tubulin was used to normalize protein loading. Representative blots from three independent experiments are shown. *D*: Densitometric quantification of liver ($n = 11$), kidney ($n = 4$), and WAT ($n = 4$) blots shown in *C*. ■, Ad-shCT; □, Ad-shPck1 group. Data are means ± SE; **$P < 0.01$, Student's *t* test. (Please see http://dx.doi.org/10.2337/db07-1087 for a high-quality digital representation of this figure.)

provides a novel therapeutic approach for the treatment of diabetes.

RESEARCH DESIGN AND METHODS

Experimental animals and adenovirus. Male C57BKS.Cg-+Lepr[db]/+Lepr[db] (*db/db*) mice were purchased from Harlan Interfarma, maintained in a constant 12-h light/dark cycle, and fed a standard rodent chow and water ad libitum. At the beginning of the experiment, animals were 6–8 weeks old. All animal protocols were approved by the ethics committee at the University of Barcelona.

Recombinant E1-E3 deficient adenovirus (serotype 5) encoding shRNA against PEPCK-C (Ad-sh*Pck1*) and *Phothinus pyralis* luciferase (Ad-shCT) (used as unspecific control sequence) were generated in the Viral Production Unit of the Center of Animal Biotechnology and Gene Therapy (UPV-CBATEG) (Bellaterra, Spain).

Adenovirus was administered by tail vein injection of 6.67×10^{10} plaque-forming units (pfu)/kg in 200 μl physiological saline. Fed blood glucose and weight were measured at 8:00 A.M. Surgery was performed under isofluorane anesthesia (Abbot). Tissues were snap-frozen in liquid nitrogen and stored at −80°C until analysis. Blood was collected by inferior cava puncture.

Peripheral insulin sensitivity. Overnight fasted mice were anesthetized, and gastrocnemius muscle, epididymal fat, and liver samples were taken at time 0 and 5 min after a 10-IU/kg insulin bolus was injected via tail vein.

Glucose and insulin tolerance tests. Glucose tolerance was assayed 7 days after treatment in 32-h-fasted mice after a 1-g/kg glucose bolus intraperitoneal injection. Insulin tolerance was determined in mice fed ad libitum, after intraperitoneal injection of 2 IU/kg bovine insulin (Sigma) at day 8 after
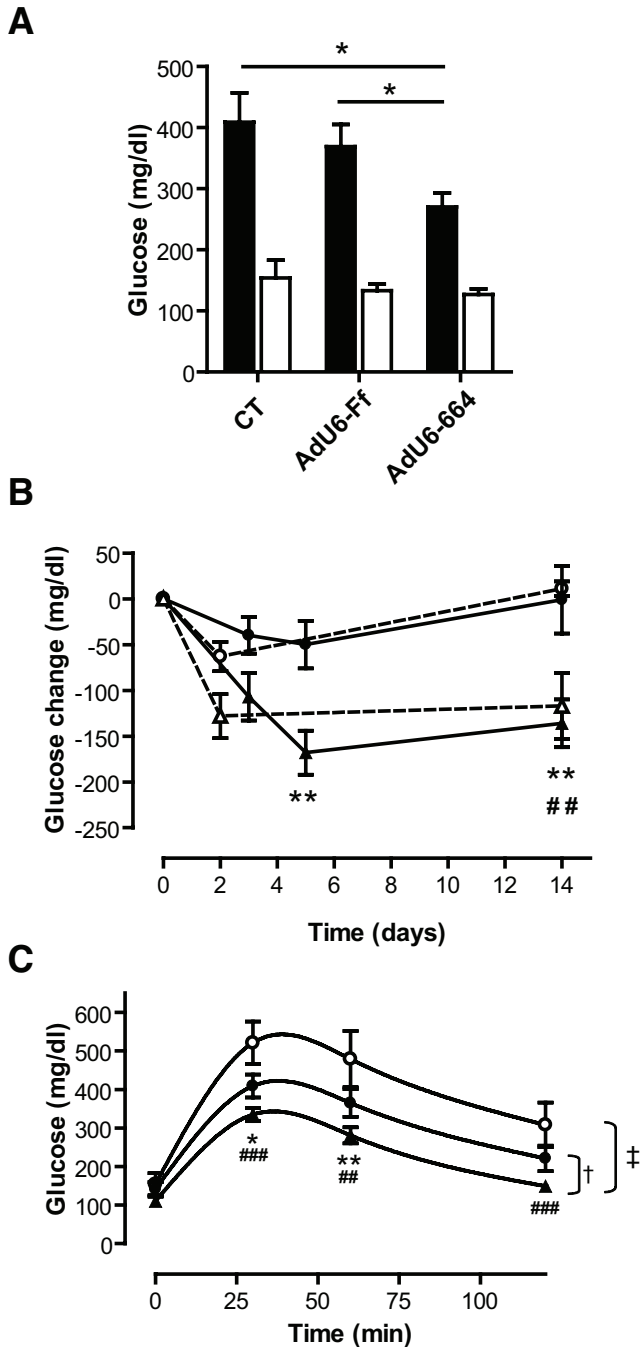
A

B

C

FIG. 2. Knocking down hepatic PEPCK-C in diabetic *db/db* mice leads to improved glucose homeostasis. *A*: Fed glycemia (■) was assessed 14 days after treatment with saline (CT; *n* = 5) with adenovirus expressing a nonspecific shRNA (Ad-shCT; *n* = 19) or with a PEPCK-C specific shRNA (Ad-sh*Pck1*; *n* = 19). Fasting glycemia was measured after a 32-h fast on day 7 after infection (□) in the same animals. Data are means ± SE; **P < 0.05, Student's *t* test. *B*: Fed glycemia relative to glycemia before treatment. Fed glycemia was scored in CT group (*n* = 5; ○), Ad-shCT (*n* = 19; ●), and Ad-sh*Pck1* (*n* = 19; ▲) before treatment and over the duration of the experiment. An additional experimental group was treated orally with metformin (MET) (*n* = 5; △). Metformin was added to drinking water to achieve a daily dose of 400 mg · kg⁻¹ · day⁻¹ in view of the daily water consumption. Average daily water consumption was calculated every day for 1 week before initialization of experiment. Water consumption and metformin dosage was recalculated twice a week and corrected, if necessary, to adjust dosage. Data are means ± SE; ***P < 0.01 Ad-sh*Pck1* vs. Ad-shCT; and ***P < 0.01 MET vs. CT, Student's *t* test. *C*: Seven days after adenoviral infection, an intraperitoneal glucose tolerance test was performed in 32-h-fasted mice as described in RESEARCH DESIGN AND METHODS, and glucose was measured at the indicated time points in CT (*n* = 5), Ad-shCT (*n* = 13), and Ad-sh*Pck* (*n* = 12) groups. **P < 0.05

treatment. Blood glucose was measured at the indicated time points after challenge.

Glucose production from pyruvate. A 2 g/kg buffered pyruvate (Sigma) bolus was injected intraperitoneally in 32-h–fasted mice on day 7 after adenoviral infection. Glucose levels were measured at indicated time points.

RNA extraction and quantitative RT-PCR. Total RNA was extracted using RNAeasy mini kit (Qiagen). cDNA synthesis from 2 μg RNA was performed using Ready-To-Go You-Prime First Strand Beads (Amersham Biosciences) with random hexamers. mRNA levels of selected genes were quantified using a Low Density Array (Applied Biosystems) in a HT7900 Real-Time RT-PCR system (Applied Biosystems). Gene expression was normalized with β-2-microglobulin as a housekeeping gene. Data analysis is based on the ΔΔCt method.

Western blot. Tissue was homogenized in radioimmunoprecipitation assay buffer supplemented with protease and phosphatase inhibitors and centrifuged at 15,000*g* for 15 min at 4°C. Western blots were performed with 20–50 μg tissue extract. Proteins were separated in 8–12% SDS-PAGE and transferred to an Immobilon membrane (Millipore). Nuclear extracts were obtained as described previously (13).

Sheep anti–PEPCK-C antiserum (a gift from Dr. Granner, Vanderbilt University, Nashville, TN) was used at a 1:20,000 dilution; antibodies against acetyl-CoA carboxylase (ACC) and ACC-P (Ser⁷⁹) (Upstate) were used at 1:2,000; and antibodies against AMP-dependent kinase (AMPK), AMPK-P (Thr¹⁷²), AKT, AKT-P (Thr³⁰⁸), AKT-P (Ser⁴⁷³) (Cell Signaling), Sirt1 (Upstate), and sterol regulatory element–binding protein 1c (SREBP-1c; Santa Cruz Biotechnology) were used at 1:1,000. Voltage-dependent anion channel (VDAC) antibody (provided by Dr. Pujol, IDIBELL) was diluted 1:1,000. Fatty acid synthase (FAS) and protein kinase C ε (PKCε) antibodies (Santa Cruz Biotechnology) were used at 1:500 dilution. FOXO1 (Santa Cruz Biotechnology), FOXO1-P (Ser²⁵⁶) (Cell Signaling), and peroxisome proliferator–activated receptor-γ coactivator (PGC)-1 (Cell Signaling) were used at 1:250. All membranes were normalized using monoclonal anti–γ-tubulin (Sigma) at 1:10,000. Horseradish peroxidase activity linked to secondary antibody was detected with ECL substrate (Pierce) in a Fujifilm LAS 3000 Intelligent Dark Box IV imaging system. Densitometry was performed using Multi Gauge software.

PKCε activity was estimated as the ratio of membrane to cytosol PKCε signal. To separate membrane and cytosolic fractions, liver homogenates were centrifuged at 800*g* for 10 min, and supernatants were further centrifuged at 100,000*g* for 45 min. Enrichment was assessed after blotting the membranes with antibodies (1:1,000) against cytosolic (pyruvate kinase [L-PK]; gift from Dr. Bartrons, University of Barcelona) and membrane-associated (epithelial growth factor receptor [EGFR], gift from Dr. Rosa, University of Barcelona) proteins.

Histology and immunofluorescence. A portion of the third hepatic lobule was fixed for at least 24 h in 4% paraformaldehyde, equilibrated in 30% saccharose, embedded in Tissue-Tek OCT compound (Sakura), and stored at −80°C until 7-μm-thick cryosections were obtained. Oil-red lipid staining and PEPCK-C immunostaining were previously described (12).

Blood and liver biochemical analysis. Blood glucose was measured using a Glucocard Memory 2 apparatus (Menarini) by tail clipping. Serum metabolites were measured in the Veterinarian Clinical Biochemistry Service, Veterinary Hospital, Universitat Autònoma de Barcelona (Barcelona, Spain). Serum insulin was determined using Ultrasensitive Mouse Insulin ELISA (Mercodia). HDL cholesterol was quantified using a Reflotron system (Roche Diagnostics).

Hepatic glycogen was measured essentially as previously described (9). Hepatic triglycerides and fatty acid content were quantified using a TAG kit (Sigma) and NEFA kit (Wako), respectively, in 3 mol/l KOH, 65% ethanol extracts, based on the method of Salmon and Flatt for liver saponification. Hepatic short chain acyl-CoAs (acetyl-CoA, malonyl-CoA, propionyl-CoA, and succinyl-CoA) were analyzed by high-performance liquid chromatography (HPLC) as described previously (14) in the Research Support Services from the University of Barcelona. Nucleotides (ATP/ADP/AMP) were determined in neutralized 10% perchloric acid extracts by HPLC.

High-resolution respirometry. O₂ consumption was measured using a high-resolution Oxygraph respirometer (Oroboros, Innsbrook, Austria) in isolated hepatocytes. Briefly, liver was preperfused with calcium-free Hanks' balanced salt solution (HBSS) buffer (Sigma) at 37°C before perfusion with Ca²⁺-containing HBSS and 3.5 mg/ml Liberase Blendzyme (Roche). Hepatocytes were cleared by repeated centrifugation at 50*g* for 5 min, and viability

Ad-sh*Pck1* vs. Ad-shCT; ***P < 0.01; and ****P < 0.001 Ad-sh*Pck1* vs. CT, Student's *t* test. A two-way ANOVA did not detect significant differences between the CT and Ad-shCT groups but demonstrated statistically significant changes when comparing the Ad-sh*Pck1* versus CT (‡*P* < 0.001) and versus Ad-shCT (†*P* < 0.05) treatment groups. Data are means ± SE.
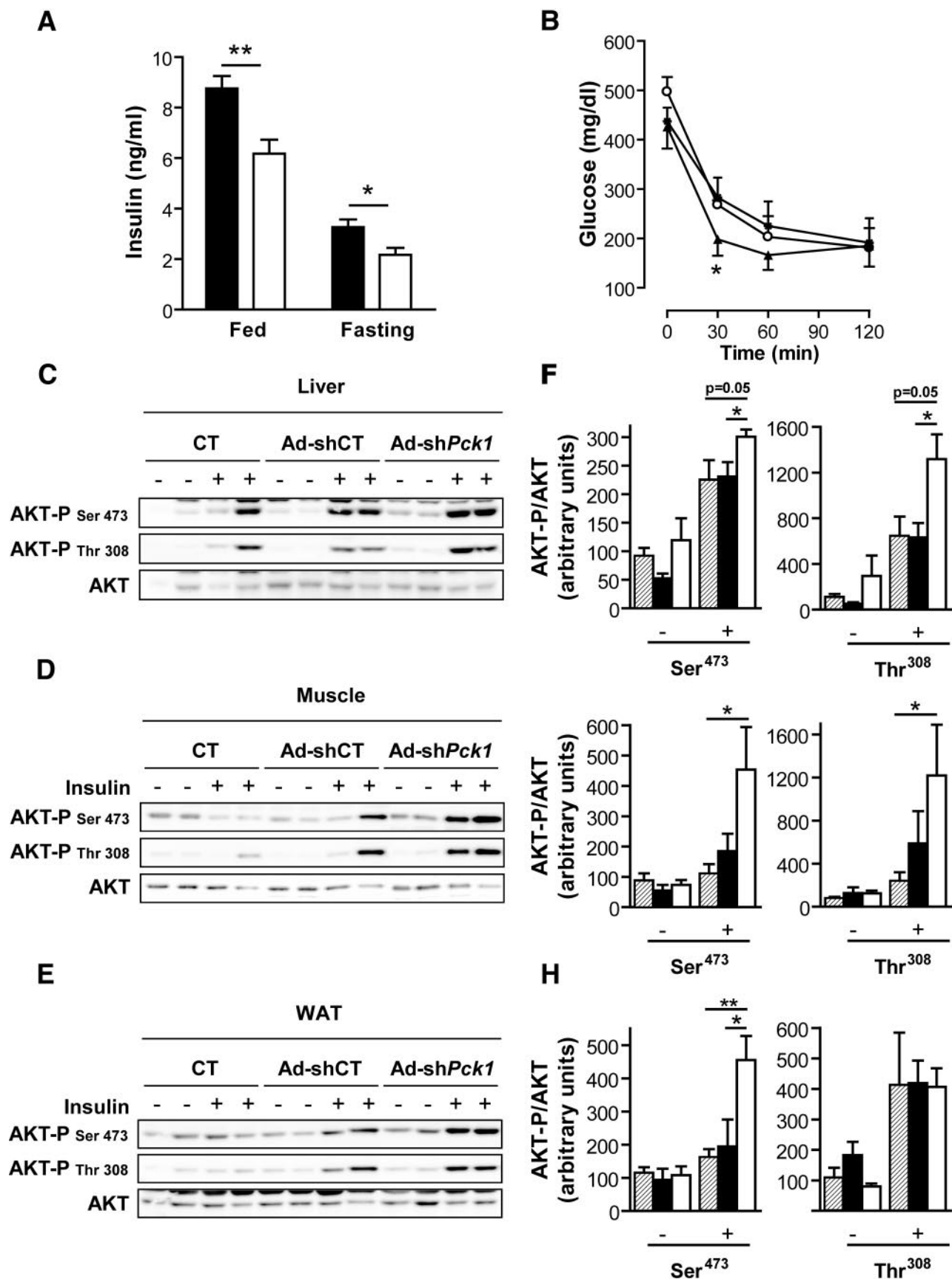
FIG. 3. Improved insulin sensitivity in hepatic PEPCK-C–silenced animals. *A*: Plasma insulin levels was assessed in fed mice 14 days after infection (Ad-shCT, $n = 5$; Ad-sh*Pck1*, $n = 4$; **$P < 0.01$, Student's t test) or in 32-h-fasted mice 7 days after infection (Ad-shCT, $n = 13$; Ad-sh*Pck*, $n = 12$; *$P < 0.05$, Student's t test). ■, Ad-shCT; □, Ad-shPck1 group. *B*: For IPITT, a 2-IU/kg insulin bolus was injected into awake fed mice. Blood glucose levels were determined at the indicated time points after insulin bolus (CT, ○, $n = 5$; Ad-shCT, ●, $n = 8$; Ad-sh*Pck1*, ▲, $n = 9$). Data are

(>80%) was assessed by trypan blue exclusion. The respiration medium consisted of F-12 Coon's modification supplemented with 20 mmol/l HEPES, 20 mmol/l lactate, 2 mmol/l pyruvate, 2 mmol/l glutamine, and 1 mmol/l octanoate conjugated with 0.5% BSA. Medium was equilibrated with air at 37°C and stirred at 750 rpm until a stable signal was obtained for calibration at air saturation. At least 10^6 hepatocytes per milliliter were used for measurements. The titration protocol, which was completed within 50–60 min, was recorded at 2-s intervals using a computer-driven data acquisition system (Datlab; Oroboros).

Statistical analysis. Results are expressed as the means ± SE. Statistical analysis was always performed by one-way or two-way ANOVA and two-tailed Student's t test. A $P < 0.05$ was considered significant.

RESULTS

Liver-specific PEPCK-C gene silencing. A previously validated shRNA sequence against PEPCK-C (12) was engineered into an adenovirus vector (Ad-shPck1) and tested for relative silencing efficiency compared with a control sequence (Ad-shCT). Treatment with Ad-shPck1 achieved a 42 and 25% reduction in Pck1 gene expression in fed and fasted livers, respectively (Fig. 1A). Interestingly, the net amount of RNA silenced was similar independent of nutritional status. Densitometric quantification of Western blots confirmed a similar amount of hepatic PEPCK-C protein reduction on treatment (100 ± 15.1 vs. 46.1 ± 6.8 relative units; $n = 11$, $P < 0.01$) (Fig. 1C and D). Because PEPCK-C is also present in kidney and adipose tissue, we assessed the tissue specificity of silencing. No changes in PEPCK-C protein content were observed either in kidney or epididymal adipose tissue (Fig. 1C and D). Finally, immunohistochemical analysis of PEPCK-C demonstrates a nonhomogeneous reduction of PEPCK-C immunoreactivity that is more evident in pericentral than periportal hepatocytes (Fig. 1B).

Whole-body glucose homeostasis and insulin sensitivity. To investigate the consequences of PEPCK-C silencing on glycemia control, key metabolic parameters were measured. Fed blood glucose was significantly reduced in Ad-shPck1 animals (271 ± 23 mg/dl) compared with both saline-treated (409 ± 48 mg/dl) and Ad-shCT–treated (370 ± 38 mg/dl) groups, although no significant changes were found in fasted animals (Fig. 2A). Interestingly, PEPCK-C silencing and oral metformin treatment demonstrated similar variations in fed glycemia (Fig. 2B).

Systemic glucose clearance, assessed using a glucose tolerance test, was improved after Ad-shPck1 treatment, as demonstrated by a reduction in the area under the curve of ~40 and 20% compared with saline-treated and Ad-shCT groups, respectively (Fig. 2C). Also, fed and fasting insulinemia were significantly reduced after treatment with Ad-shPck1 (Fig. 3A). Accordingly, an intraperitoneal insulin tolerance test showed that PEPCK-C–silenced animals have higher sensitivity to insulin (Fig. 3B). Furthermore, Ad-shPck1–treated animals scored significantly lower (2.38 ± 0.01, $n = 14$ vs. 2.74 ± 0.07, $P < 0.01$, $n = 5$ and vs. 2.53 ± 0.01, $P < 0.05$, $n = 14$; Ad-shPck1 vs. saline

means ± SE, *$P < 0.05$ (CT vs. Ad-shPck1) and $P = 0.09$ (Ad-shCT vs. Ad-shPck1), Student's t test. Insulin signaling in liver (C and F), muscle (D and G), and epididymal fat depots (E and H) was assessed in overnight fasted mice 1 week after infection by means of an intravenous insulin bolus (10 IU/kg) as described in RESEARCH DESIGN AND METHODS. The level of AKT phosphorylation (at both Ser[473] and Thr[308] residues) and the total AKT protein content were detected by Western blot (C–E). Representative blots of two independent experiments are shown. Additionally, bands were quantified by densitometry (F–H). ▨, saline-injected animals (CT); ■, Ad-shCT group; □, Ad-shPck1 group. Bars represent the AKT-P–to–AKT ratio related to control (CT) group in the basal state. Data are means ± SE of 4–6 animals per group. *$P < 0.05$ and **$P < 0.01$, Student's t test.

TABLE 1
Metabolic profile of db/db mice after partial liver silencing of PEPCK-C

		Blood metabolites						Liver metabolites		
		FFA (mmol/l)	TAG (mg/dl)	β-HBA (mmol/l)	GPT (units/l)	Total cholesterol (mg/dl)	HDL cholesterol (mg/dl)	Glycogen (mmol · l⁻¹ · g⁻¹)	TAG (mg/g)	Fatty acids (mmol/g)
Fed	Ad-shCT	0.92 ± 0.05	174.75 ± 12.61	0.22 ± 0.05	144.00 ± 11.46	116.53 ± 3.16	60.86 ± 5.23	273.41 ± 31.34	117.37 ± 15.20	0.48 ± 0.28
	Ad-shPck1	0.78 ± 0.04	117.83 ± 12.61*	0.29 ± 0.04	150.82 ± 4.99	133.27 ± 4.60†	74.93 ± 4.75*	296.74 ± 18.65	173.39 ± 11.43†	1.68 ± 0.45*
Fasted	Ad-shCT	0.89 ± 0.08	134.50 ± 11.05	0.40 ± 0.05	253.33 ± 17.99	104.85 ± 3.06	ND	70.18 ± 3.33	43.94 ± 4.75	2.30 ± 0.21
	Ad-shPck1	0.58 ± 0.02	86.00 ± 7.14	0.66 ± 0.08	205.67 ± 5.27	132.85 ± 2.07‡	ND	19.41 ± 3.69§	107.05 ± 11.24§	4.01 ± 0.27§

Data are means ± SE. $n = 13–16$ (Ad-shCT), $n = 15–18$ (Ad-shPck1), $n = 6$ (Ad-shCT and Ad-shPck1). *$P < 0.05$; †$P < 0.01$ vs. control virus treatment in fed experiments; unpaired Student's t test. ‡$P < 0.01$; §$P < 0.001$ vs. control virus treatment in fasting experiments; unpaired Student's t test. ND, nondetermined. Sera were obtained 14 days after adenoviral infection from fed or overnight-fasted mice. GPT, glutamic pyruvic transaminase.

treated and vs. Ad-shCT, respectively) when their degree of insulin resistance was assessed from the QUICKI index (15).

Next, we directly evaluated insulin signaling in vivo measuring insulin-stimulated AKT phosphorylation in liver, muscle, and epididymal adipose tissue (white adipose tissue [WAT]). AKT phosphorylation at Ser^{473} and Thr^{308} was enhanced in Ad-sh*Pck1*–treated animals after insulin treatment, in marked contrast to reduced signaling by insulin in saline-treated and Ad-shCT–treated groups (Fig. 3*C–H*). These data demonstrate improved peripheral insulin sensitivity after partial hepatic PEPCK-C knockdown in the *db/db* mouse model.

Gluconeogenesis and HGO. HGO, determined by the flux from pyruvate to glucose in vivo, was reduced in Ad-sh*Pck1*–treated animals (Fig. 4*A*). Moreover, liver glycogen was significantly reduced in Ad-sh*Pck1*–treated animals on fasting (Table 1), consistent with decreased hepatic glucose production capacity

Glucose-6-phosphatase catalyzes the last step in the gluconeogenic and glycogenolysis pathways, and is, therefore, responsible for regulating HGO. The mRNA of this enzyme (encoded by *G6pc*) was significantly reduced at levels comparable with those observed for PEPCK-C (encoded by *Pck1*). Glucose-6-phosphatase and PEPCK-C are regulated by transcription factors like hepatocyte nuclear factor-4α (HNF-4α) (encoded by *Hnf4α*) and FOXO1, which are co-activated by PGC-1α (encoded by *Ppargc1α*). PGC-1α mRNA was slightly reduced in PEPCK-C–silenced animals (Fig. 4*B*), although PGC-1α protein in nuclear extracts was constant (Fig. 4*C* and *D*). HNF-4α is down-regulated, albeit nonsignificantly, in treated animals. In addition, FOXO1 phosphorylation at Ser^{256} increased in liver of Ad-sh*Pck1*–treated animals (Fig. 4*E* and *F*). These data suggest that insulin signaling through AKT-dependent FOXO1 phosphorylation contributes to the observed reduction in steady-state mRNA levels for gluconeogenic genes such as *G6pc* and *Pck1*.

Lipid homeostasis. To investigate the effects of liver-specific PEPCK-C knockdown on lipid metabolism, several blood and liver parameters were analyzed. Serum triglycerides were pronouncedly reduced both in fed and fasted animals after PEPCK-C silencing in the liver, accompanied by decreased serum free fatty acids (FFAs) and increased β-hydroxybutyrate. Furthermore, a net increase in total serum cholesterol with a concomitant increase in HDL cholesterol was found (Table 1).

Lipid accumulation in the liver is a characteristic of the diabetes phenotype in *db/db* mice. Oil-red staining demonstrated both micro- and macrovesicular lipid droplets in Ad-shCT–treated livers, which are more profuse in Ad-sh*Pck1* group, especially in periportal compared with perivenous hepatocytes (Fig. 5*A*). Consistently, we observed a moderate increase in hepatic triacylglycerol (TAG) and a 3.5-fold increase in liver fatty acid content after PEPCK-C silencing (Fig. 5*B*). Meanwhile, the level of FAS mRNA was unaltered, whereas SREBP1-c and liver X receptor-α decreased ~25% (Fig. 5*C*). Correspondingly, the precursor (p125) and active form (p68) of SREBP1-c were reduced, whereas FAS protein content was unchanged (Fig. 5*D* and *E*). Moreover, mRNA and protein levels from glycolytic and lipogenic enzymes, such as glucokinase (*Gck*), L-PK, or malic enzyme (*Mod1*), were unaltered or significantly reduced (Fig. 5*C–E*). ChREBP, which plays an important role in regulating glycolytic (L-PK) and lipogenic (ACC and FAS) genes, was unaltered

(Fig. 5*C–E*), which supports the absence of de novo lipogenesis in livers of Ad-sh*Pck1*–treated mice.

Malonyl-CoA is an important contributor to the opposing regulation of fatty acid β-oxidation and fatty acid synthesis through its dual function as allosteric inhibitor of CPT-1 and FAS substrate (16). Although a significant increase of malonyl-CoA content in liver was found (Table 2), ACC, the enzyme responsible for its synthesis, was not stimulated because the ratio of ACC-P to ACC was unchanged in the liver of PEPCK-C–silenced mice (Fig. 5*F*). These data further support the view that PEPCK-C silencing in the liver of *db/db* mice does not induce net de novo lipogenesis.

Interestingly, despite liver lipidosis (Fig. 5*A* and *B*), hepatic and peripheral insulin signaling was improved in PEPCK-C–silenced animals (Fig. 3). PKCε plays a critical role in mediating fat-induced hepatic insulin resistance (17). No activation of PKCε was observed after partial PEPCK-C knockdown in *db/db* livers (Fig. 5*G* and *H*), suggesting that lipid accumulation is dissociated from insulin resistance induction in our model.

Modulation of energy metabolism. Because impairment of the tricarboxylic acid (TCA) cycle and mitochondrial function are hallmarks of liver-specific PEPCK-C knockout mice (6,8,9), we evaluated several parameters of mitochondrial function, including β-oxidation. The rate-limiting step in β-oxidation is the transport of acyl-CoA into the mitochondria catalyzed by the CPT-1 shuttle, whose mRNA content was slightly reduced (Fig. 6*B*). Consistently, the mRNA for PGC-1α, a key player in the regulation of both β-oxidation and gluconeogenic pathways, was lowered after treatment (Fig. 4*B*). In contrast, a slight increase in serum ketones in both fed and fasted animals (Table 1), together with unchanged levels of HMG-CoA synthase mRNA (Fig. 6*B*) and a significant increase in propionyl-CoA, an odd chain β-oxidation intermediate (Table 2), suggests that β-oxidation was not markedly affected.

The mitochondrial respiration rate, determined in freshly isolated hepatocytes in the presence of octanoate, was unaffected by treatment with Ad-sh*Pck1*. Moreover, the maximum mitochondrial respiration capacity (uncoupler carbonyl cyanide *p*-trifluoromethoxyphenyl-hydrazone [FCCP]) (Fig. 6*A*) and the content of the inner mitochondrial membrane ADP transporter VDAC (Fig. 6*C*), a marker of the amount of respiratory chains and hence mitochondrial content, were unchanged, suggesting that partial PEPCK-C knockdown does not impair the TCA cycle and does not negatively affect mitochondrial biogenesis or limit mitochondrial oxidative capacity in excess of medium-chain fatty acid substrate. Consistently, no accumulation of TCA intermediates, like acetyl-CoA and succinyl-CoA, was observed (Table 2). Additionally, the expression profile of cytosolic (decreased) and mitochondrial (unaltered) superoxide dismutases (SODs) is compatible with increased peroxisomal oxidation activity (18) (Fig. 6*D*). The ratios estimated from respirometry data (respiratory control ratio [RCR], uncoupling control ratio [UCR], and phosphorylation RCR [RCRP]) were unaltered after Ad-sh*Pck1* treatment (Fig. 6*A*). In agreement with UCR index, the level of expression from the gene encoding the uncoupling protein two (*Ucp2*) was unchanged, suggesting that mitochondrial respiration was not uncoupled (Fig. 6*B*).

It is widely accepted that gluconeogenesis is dependent on fatty acid oxidation as an energy source. An imbalance between these two pathways would, theoretically, alter
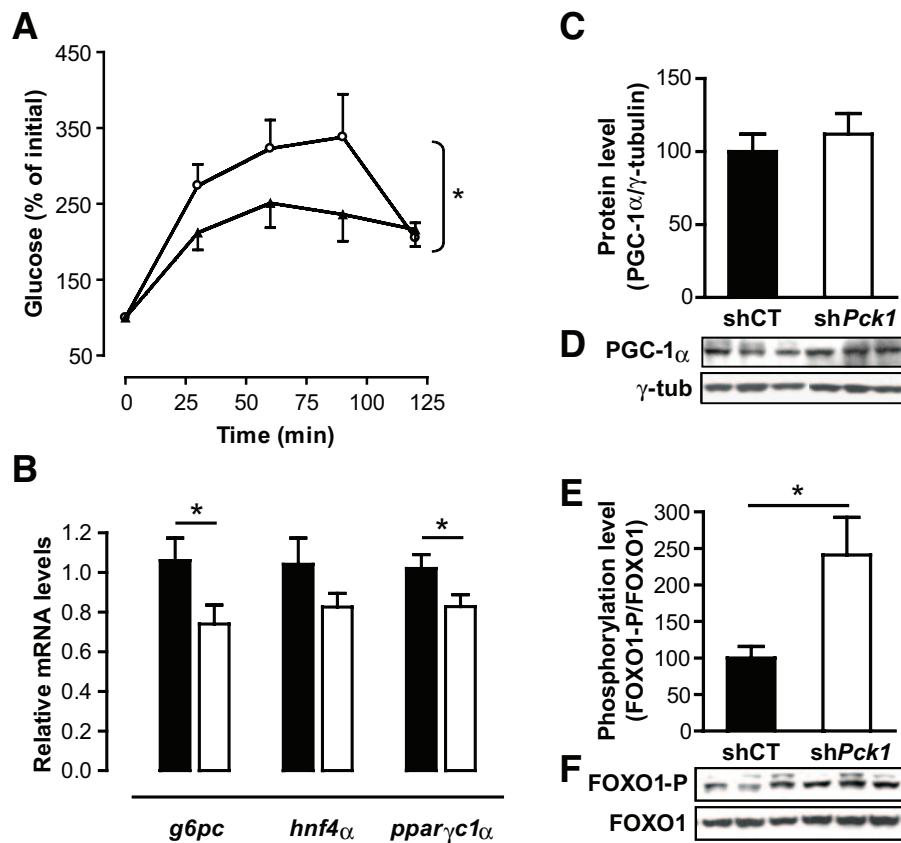
FIG. 4. Coordinated downregulation of gluconeogenic genes and decreased hepatic glucose production capacity after hepatic PEPCK-C silencing. *A*: HGO was evaluated in vivo by assaying the glucose production from pyruvate as described in RESEARCH DESIGN AND METHODS. Hepatic PEPCK-C–silenced group reflected a significant reduction in glucose production capacity after a pyruvate bolus injection. Two-way ANOVA was used to discriminate treatment efficiency. Data are means ± SE. Ad-shCT, ○, $n = 9$; Ad-sh*Pck1*, $n = 9$, ▲; *$P < 0.05$. *B*: Expression of significant genes involved in gluconeogenesis (*G6pc*, *Hnf-4α*, and *Ppargc1α*) was examined 2 weeks after treatment with Ad-shCT ($n = 10$; ■) or Ad-*shPck1* ($n = 11$; □) in fed animals. Gene expression was quantified using quantitative RT-PCR in an Applied Biosystems 7900HT Micro Fluidic Card. Data analysis was performed using the ΔΔCt method and β-2-microglobulin as housekeeping gene. Each value represents the mean relative amount of mRNA with respect to that in the control experimental treatment. Student's *t* test was used to determine statistical differences between treatments. *$P < 0.05$, Student's *t* test. *C*: Western blot immunodetection of PCG-1α in hepatic nuclear extracts obtained from fed mice 14 days after treatment. Representative blots are shown. *D*: Densitomentric quantification of PGC-1α protein content in blots shown in *C* are represented as PGC-1α content relative to γ-tubulin, which was used to normalize protein charge. Data are means ± SE, $n = 6$. *E*: Phosphorylation level of FOXO1 at the Ser^{256} residue was analyzed by Western blot in total homogenates of livers from fed mice 14 days after treatment. Total FOXO1 content was used to normalize phosphorylation level. *F*: Densitometric quantification of blots represented in *E*. Phosphorylation level is represented as FOXO1–to–phospho-FOXO1 Ser^{256} ratio relative to control group. ■, Ad-shCT; □, Ad-sh*Pck1* group. $n = 10$, *$P < 0.05$, Student's *t* test.

cellular energy charge (CEC), unless a corresponding energy producing or consuming pathway compensates for such disequilibrium. Our data show an apparent reduction in gluconeogenesis while β-oxidation is maintained. Consistently, CEC was greatly increased because of a 25% reduction of AMP and a 50% increment in ATP content (Table 2). As a result, the master-switch energy sensor AMPK (19), which is activated by decreasing energy charge, was not stimulated, as determined by the ratio of phosphorylated versus total AMPK (Fig. 6*E*), and ACC, a target for AMPK, was not inhibited by phosphorylation (Fig. 5*D*).

The work of Rodgers et al. (20) sheds some light on the regulation of gluconeogenesis in response to nutrients and changes in redox potential mediated by Sirt1, a NAD^+-dependent deacetylase involved in PGC-1α activation. Therefore, we evaluated the levels of Sirt1 to investigate whether the pathway could be responsible for the coordinated reduction in gluconeogenic enzymes and regulatory factors. A reduction of ~50% ($100 ± 9.16$ vs. $47.03 ± 10.19$; $n = 7$; $P < 0.001$; Student's *t* test) in the levels of Sirt1 protein in the liver was observed (Fig. 6*F–G*).

DISCUSSION

The natural tropism of adenovirus for the liver was used to obtain efficient, organ-specific delivery of a shRNA-producing expression vector against PEPCK-C. Infection of *db/db* mice with adenovirus-directed shRNA allowed inhibition of PEPCK-C specifically in the liver, with unaltered levels in kidney and WAT, where PEPCK-C has important roles in gluconeogenesis from glutamine and glyceroneogenesis, respectively (3).

Inmunostaining experiments show a PEPCK-C gradient across the porto-central axis of the liver acinus (21). Silencing efficiency was higher in the perivenous portion of the acinus (Fig. 1*C*), where PEPCK-C levels are lower. Although similar silencing pattern and efficiency (~50%) was obtained in our previous study on type 1 diabetes (12) using a hydrodynamic gene transfer technique, the present report demonstrates that the use of adenovirus can result in an absolute higher silencing efficiency (Supplementary Fig. 1, which is detailed in an online appendix [available at http://dx.doi.org/10.2337/db07-1087]) and longer lasting effects (up to 2 weeks), which allowed us to evaluate the
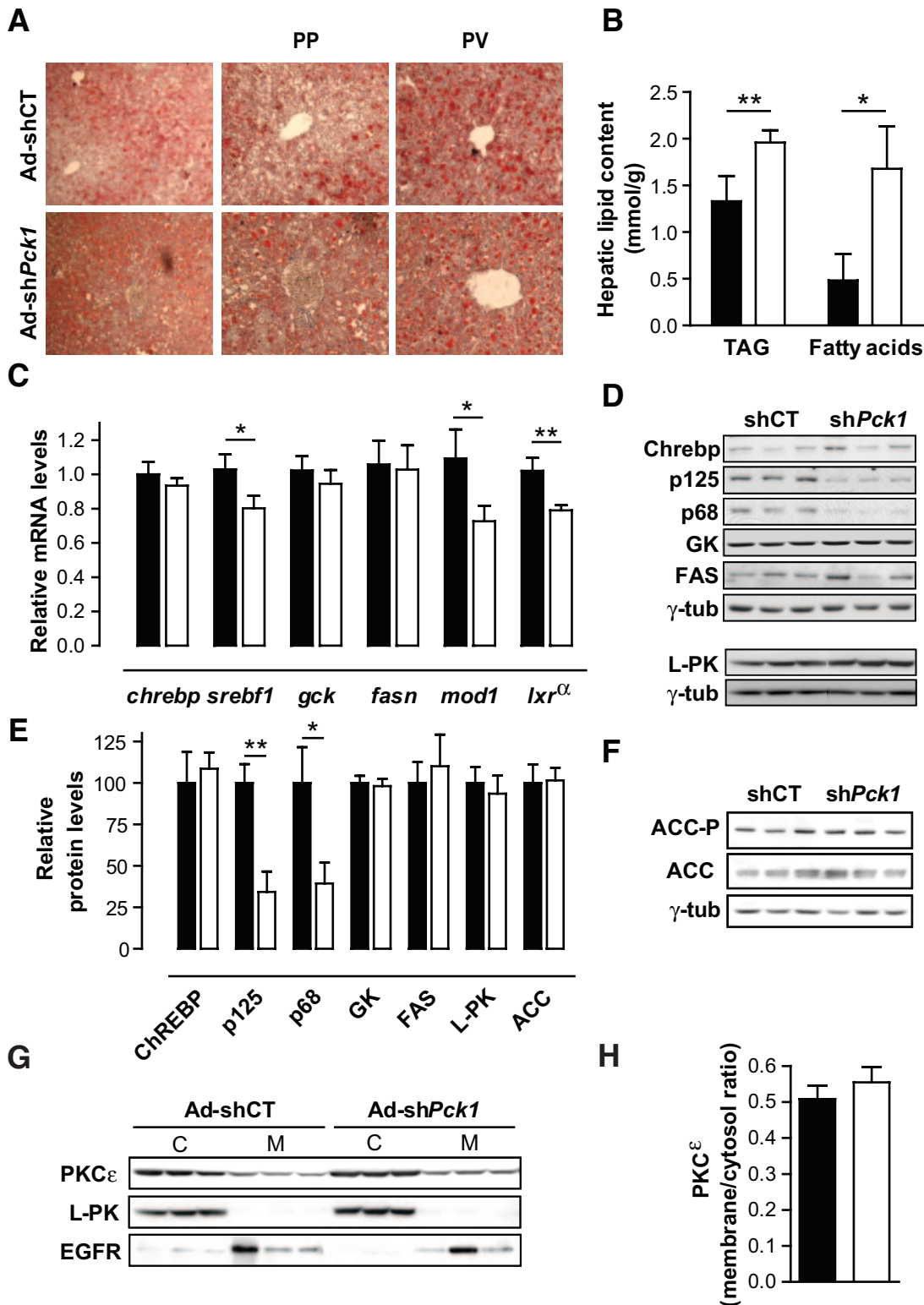
FIG. 5. Effect of hepatic PEPCK-C partial silencing on hepatic lipid homeostasis. *A*: Livers from fed mice 14 days after treatment were fixed in 4% paraformaldehyde, and oil-red staining was performed in 7-μm cryosections. *Right panel* shows a ×100 magnification liver section. A view of periportal (PP) and perivenous (PV) zones are shown with a ×200 magnification. Representative pictures from three independent experiments are shown. *B*: Triglyceride and fatty acid content in fed livers from unspecific shRNA (Ad-shCT; ■; *n* = 14) or PEPCK-C–targeted (Ad-sh*Pck1*; □; *n* = 16) treatment. Data are means ± SE; *$P < 0.05$, **$P < 0.01$. *C*: Expression of significant genes involved in glycolysis and lipogenesis (*fasn*, *srebf1*, *chrebp*, *mod1*, *gck*, and *lxr-α*) was examined. Livers were obtained in fed state 14 days after infection with Ad-shCT (*n* = 10; ■) or Ad-sh*Pck1* (*n* = 11; □). Gene expression was quantified by quantitative RT-PCR using Applied Biosystems 7900HT Micro Fluidic Card, and data were analyzed using the ΔΔCt method and β-2-microglobulin as housekeeping gene. Each value represents the mean relative amount of mRNA with respect to that in the control experimental treatment. *$P < 0.05$, **$P < 0.01$, Student's *t* test. *D*: Protein levels of glycolytic and lipogenic enzymes and transcription factors in livers from fed animals 14 days after treatment were analyzed by Western blot from total liver extracts. Blots are representative of three independent experiments. *E*: Densitometric quantification of blots represented in *D* and *F*. Data are means ± SE, *n* = 5–19; *$P < 0.05$, **$P < 0.01$, Student's *t* test. ■, Ad-shCT group; □, Ad-shPck1 group. *F*: Western blot analysis of ACC protein content and phosphorylation levels (ACC-P Ser[79]) in fed livers from Ad-shCT and Ad-sh*Pck1* groups. Blots were normalized with γ-tubulin. Representative

TABLE 2
Nucleotide and short-chain acyl-CoA content in fed *db/db* livers

	AMP (μmol/g)	ADP (μmol/g)	ATP (μmol/g)	CEC	Acetyl-CoA (nmol/g)	Propionyl-CoA (nmol/g)	Succinyl-CoA (nmol/g)	Malonyl-CoA (nmol/g)
Ad-shCT	1.05 ± 0.06	1.24 ± 0.08	1.02 ± 0.08	0.47 ± 0.01	140.13 ± 1.95	48.12 ± 0.84	31.44 ± 3.12	2.079 ± 0.239
Ad-sh*Pck1*	$0.77 \pm 0.11*$	1.16 ± 0.07	$1.47 \pm 0.17†$	$0.54 \pm 0.02†$	130.29 ± 2.47	$56.68 \pm 1.25†$	31.31 ± 2.10	$4.472 \pm 0.932*$

Data are means $\pm$ SE. $n = 8$. $*P < 0.05$; $†P < 0.01$ vs. control virus treatment; unpaired Student's t test. Tissue was obtained 14 days after treatment. CEC = (ATP + 1/2 AMP)/(ATP + ADP + AMP).

metabolic impact and underlying mechanisms of knocking down hepatic PEPCK-C in a type 2 diabetes model.

Mice with reduced PEPCK-C liver content showed a clear improvement in glucose tolerance and fed glycemia, comparable with the results of oral metformin treatment. However, fasting glucose was unchanged, even though HGO from pyruvate was clearly reduced. Compensatory HGO from glycogenolysis, as supported by reduced hepatic glycogen content in fasting and even in fed animals when silencing reached 90% (Supplementary Fig. 1), could be responsible for unchanged fasting glycemia. Accordingly, fasting glycemia was significantly reduced in treated animals when PEPCK-C was 90% silenced (Supplementary Fig. 1).

Improved glucose tolerance and insulinemia suggest increased peripheral insulin sensitivity. Lower insulin levels could be secondary to reduced glycemia; however, phloridzin treatment, which inhibits intestinal glucose uptake and renal reabsorption, has been shown to reduce glycemia with no effects on insulin sensitivity in a type 2 diabetes mouse model (22). Moreover, an ameliorated intraperitoneal insulin tolerance test (IPITT) and higher insulin-stimulated AKT phosphorylation in muscle and adipose tissue strongly support the hypothesis of an insulin-sensitizing effect. In adipose tissue, AKT phosphorylation at Thr 308 was unchanged by either treatment. However, it has been shown that insulin-stimulated glucose uptake is independent of signaling through Thr[308] and closely matches Ser[473] AKT-P levels (23). The QUICKI index was also suggestive of an overall reduction in insulin resistance. In addition, hepatic PEPCK-C silencing improves clinical symptoms of type 2 diabetes, such as polydipsia, polyuria, and glycosuria, as revealed by metabolic cage studies (data not shown). Cross talking between liver and brain through the vagal nerve (24) could be responsible for a coordinated metabolic regulation in peripheral tissues in response to hepatic energy metabolism modulation, affecting systemic insulin sensitivity (25).

Interestingly, despite hepatic lipid accumulation, AKT phosphorylation was also evident in the liver of PEPCK-C–silenced mice. Hepatic lipidosis is commonly associated with the induction of insulin resistance through incompletely understood mechanisms. Recent reports have demonstrated that lipid-induced hepatic insulin resistance is not mediated by fatty acid or TAG accumulation per se (26,27). Instead, diacylglycerol induces insulin resistance via activation of PKCε translocation to the vicinity of insulin receptor substrate-2 (17). In agreement with AKT phosphorylation data, we have observed that PKCε is not

modulated by PEPCK-C silencing, reinforcing the current view that lipid accumulation is not necessarily linked to insulin resistance in the liver.

Dislipidemia is associated with obesity and insulin resistance in type 2 diabetes (28). PEPCK-C silencing resulted in reduced plasma TAG, together with an important elevation of hepatic lipids, mainly nonsterified fatty acids. An important but not sufficiently appreciated role for PEPCK-C in the liver is glyceroneogenesis: the provision of glycerol-3-phosphate to sustain fatty acid re-esterification for triglyceride synthesis (29,30). Therefore, PEPCK-C silencing could induce a significant reduction in fatty acid re-esterification activity. How to reconcile a concomitant increase in liver TAG and a reduction of TAG in plasma is not apparent. However, elevated fatty acids in the liver could be originated from excess import, reduced oxidation, and/or increased de novo synthesis. Results presented above support that PEPCK-C–silenced livers maintain mitochondrial function. Long- and medium-chain fatty acid oxidation are highly regulated through PEPCK-C import into the mitochondria at the level of CPT-1. Reduced CPT-1 mRNA levels in PEPCK-C–silenced animals, together with increased malonyl-CoA content, a potent allosteric inhibitor of CPT-1, provide indirect evidence for a slight inhibition of fatty acid oxidation. However, this allosteric inhibition can be overridden by fatty acid abundance (31,32). Moreover, it is clear from our data that no blockade at the level of mitochondria is responsible for the accumulation of fatty acids because O_2 consumption in the presence of octanoate, which is imported into mitochondria independently of CPT-1, is unaffected in PEPCK-C–silenced hepatocytes. Also, increased plasma ketones and cellular propionyl-CoA is suggestive of maintained mitochondrial and increased peroxisomal oxidation. Actually, after a low-dose ciprofibrate-mediated peroxisome proliferation, SOD expression is modulated with a similar pattern to that observed in our model (18).

The contribution of de novo lipogenesis to the accumulation of TAG and fatty acids seen in livers of Ad-sh*Pck1* treated mice can also be discarded. Key regulatory factors involved in lipogenesis were either maintained (ChREBP) or reduced (SREBP1c and LXR-α). Lipogenic enzymes regulated by these factors (ACC and FAS) were unaltered, suggesting a main contribution of ChREBP in gene expression regulation of these targets. Whether liver glucokinase (GK) might be a target gene for SREBP1c-mediated induction has remained controversial (33,34). Our data revealed no alteration on GK mRNA or protein levels, suggesting that the LXR-α/SREBP1c axis is not directly regulating GK

blots from three independent experiments are shown. *G*: Liver cytosolic and membrane fraction were isolated as described in RESEARCH DESIGN AND METHODS. Membrane and cytosol fractions (50 μg) were loaded in a 10% SDS-PAGE. PKCε protein content in each fraction was detected by Western blot. Cellular fraction enrichment was assessed with immunodetection of membrane (EGFR) and cytosolic (L-PK) proteins. Representative blots are shown. *H*: Densitometric quantification of blots shown in *G* demonstrates unaltered membrane translocation from cytosol of PKCε after PEPCK-C silencing. Data are means ± SE, $n = 6$. ■, Ad-shCT; □, Ad-sh*Pck1* group. (Please see http://dx.doi.org/10.2337/db07-1087 for a high-quality digital representation of this figure.)

A

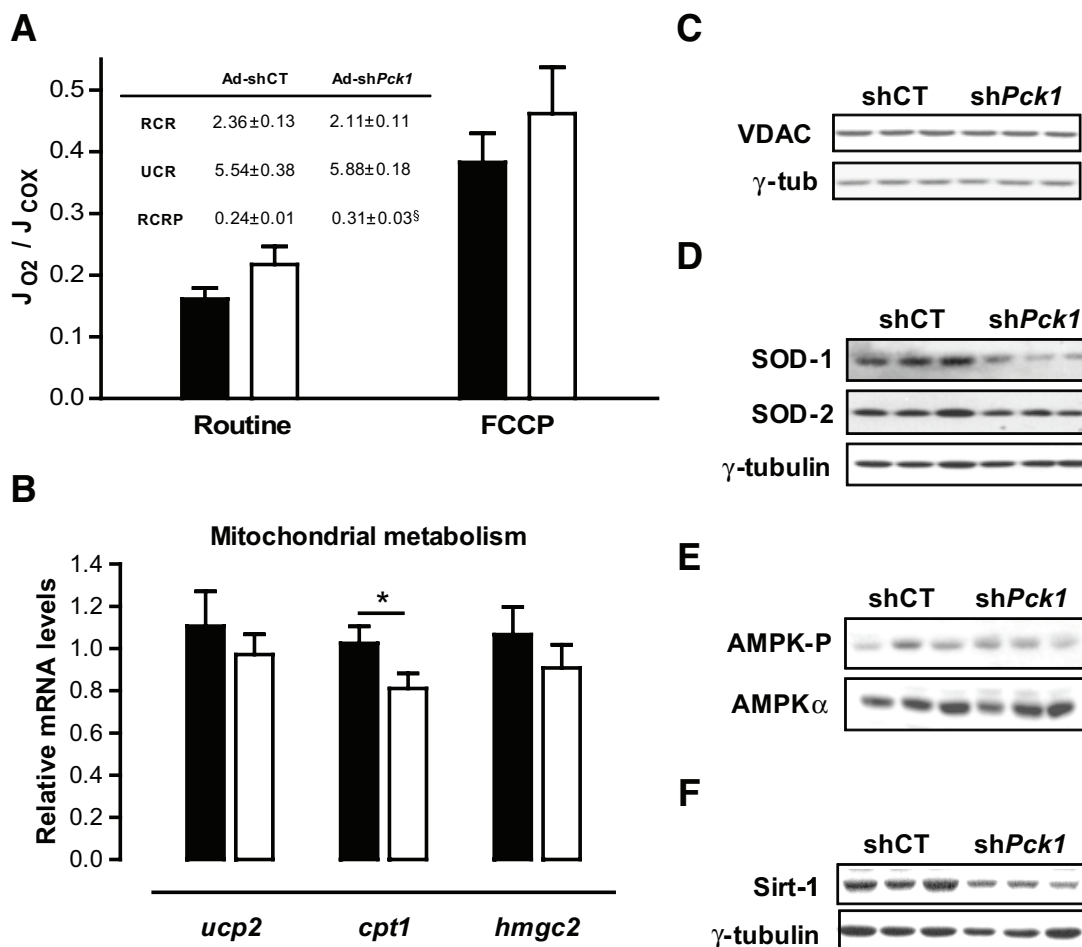|	Ad-shCT	Ad-sh*Pck1*
RCR	2.36±0.13	2.11±0.11
UCR	5.54±0.38	5.88±0.18
RCRP	0.24±0.01	0.31±0.03[§]

B

C

D

E

F

G

FIG. 6. Energy homeostasis in the liver in response to PEPCK-C silencing. *A*: High-resolution respirometry in isolated hepatocytes from fed mice 14 days after infection with Ad-shCT (■) or Ad-sh*Pck1* (□) was measured in gluconeogenic medium as described in RESEARCH DESIGN AND METHODS. Measurements of the different mitochondrial chain respiratory states were as follows: Routine respiration was measured in the presence of octanoate, followed by the inhibition of ATP synthase with 1 μg/ml oligomycin, and uncoupled respiration was initiated by the addition of 1 μmol/l FCCP followed by 5 μmol/l antimycin A to stop respiration. Finally, cytochrome c oxidase (COX) activity (J_{COX}) was measured in the presence of 2 mmol/l ascorbate and 500 μmol/l *N,N,N′,N′*-tetramethyl-p-phenylenediamine in each sample. COX activity measurements served as internal measurement normalization. *Inset*: Respiratory indexes (44) were calculated as follows: RCR, an indicator of the extent of respiration uncoupling, is the quotient between fully uncoupled respiration (FCCP) and the respiration in the presence of oligomycin. UCR, an estimate of the respiratory capacity reserve, is the quotient between fully uncoupled respiration (FCCP) and routine respiration (octanoate). Finally, RCRP, a coefficient indicating the portion of respiratory capacity applied to ATP synthesis, is calculated by subtracting oligomycin respiration from routine respiration and dividing by FCCP respiration. Data are means ± SE (*n* = 5). [§]*P* = 0.06, Student's *t* test. *B*: Expression of significant genes involved in mitochondrial function (*ucp2*, *cpt1*, and *hmgc2*) was examined in fed Ad-shCT (*n* = 10; ■) or Ad-sh*Pck1* (*n* = 11; □) animals. Total RNA was extracted with RNAeasy mini kit (Qiagen). cDNA synthesis was performed using Ready-To-Go You-Prime First Strand Beads (Amersham Biosciences) with random hexamers. Gene expression was quantified by quantitative RT-PCR using Applied Biosystems 7900HT Micro Fluidic Card, and data were analyzed using the ΔΔCt method. Gene expression was normalized using β-2-microglobulin as housekeeping gene. Values represent the mean relative amount of mRNA with respect to that in the control experimental treatment (Ad-shCT). *P* < 0.05, Student's *t* test. *C*: Mitochondrial inner membrane ADP transporter content VDAC, detected by Western blot, was used as indicator of mitochondrial respiratory chain content. *D*: Cellular protein content of the cytosolic (SOD-1) and mitochondrial (SOD-2) forms of SOD were used as indicators of cellular oxidative stress after hepatic PEPCK-C silencing as detected by Western blot. Representative blots are shown. *E*: Western blot analysis of AMPK protein content and phosphorylation levels (AMPK-P Thr[172]) in fed livers from Ad-shCT and Ad-sh*Pck1* groups. *F*: Sirt1 protein levels in fed livers form control (Ad-shCT) or PEPCK-C silencing adenovirus (Ad-sh*Pck1*) animals were estimated by Western blotting. All blots were normalized using γ-tubulin. Representative blots from three independent experiments are shown. *G*: Densitometric quantification of Sirt1 protein content in fed livers performed from blot shown in *F* confirms a significant reduction of the protein in Ad-sh*Pck1* (□) compared with Ad-shCT (■) treatment group. Data are means ± SE, *n* = 6; ****P* < 0.001, Student's *t* test.

in our model, in agreement with results obtained by Mitro et al. (35) using a LXR-α agonist.

Fatty acid uptake and activation could instead contribute to the liver fat accumulation and to decreased serum TAG and FFA. FFA import and activation into the liver is an ATP-consuming step that could be sustained by the

increased CEC. Therefore, lipid accumulation in the liver might be multifactorial, involving increased uptake from peripheral fat stores and reduced triglyceride synthesis, VLDL assembly, and export.

Liver-specific knockout animals are euglycemic and able to bypass the complete absence of PEPCK-C activity in

their livers with extrahepatic gluconeogenesis (8). Burgess et al. (36) have presented data demonstrating a weak flux control coefficient for gluconeogenesis in partial PEPCK-C knockout mice, suggesting that other factors like TCA cycle flux could contribute to gluconeogenic flux independent of PEPCK protein content. Because PEPCK-C is not only required for gluconeogenesis and glyceroneogenesis but also for cataplerosis (i.e., the removal of citric acid cycle anions), the failure of this process would result in an impairment in the TCA cycle and mitochondrial function in the liver, leading to decreased β-oxidation and oxygen consumption, together with a complete derangement in energy metabolism (6,8,9,36). Data presented in this manuscript, together with our previous study in streptozotocin-induced diabetic animals (12), demonstrate that a 50% reduction of PEPCK expression results in reduced HGO and glycemia. In addition, mitochondrial respiration and CPT-1–independent β-oxidation of fatty acids is not affected, suggesting that TCA cycle flux was sustained as long as intermediates (acetyl-CoA and succinyl-CoA) were not accumulated and ketones were overproduced. The discrepancy among the various studies might be related to one of three factors. First, knockout mice have a complete ablation of the PEPCK-C gene in the liver, in contrast to the partial reduction in the enzyme described in this study. In fact, 90% reduction in PEPCK-C protein levels in the liver, obtained with higher adenoviral dosage (Supplementary Fig. 1), reproduce the blockade on mitochondrial function observed in the knockout mice (36). Second, adaptation to a lack of PEPCK-C in knockout animals as a consequence of deletion of the gene very early during development (37) may induce a compensatory increase in gluconeogenesis in tissues other than the liver. In this regard, a recent study points to a disparity between results obtained from a liver *Ppar-α* knockout mouse and a short-term knockdown model using chemically modified siRNA against *Ppar-α* (38). Third, studies on liver-specific knockout mice were directed toward understanding the physiological role of PEPCK-C in the liver. To our knowledge, liver PEPCK-C knockout animals have not been previously studied in relevant models of diabetes, such as the one presented in this study.

The coordinated regulation of several key players in energy homeostasis in the livers of Ad-sh*Pck1*–treated animals is an intriguing observation. We have identified Sirt1 as a probable mediator in the response of the cell to a partial reduction in PEPCK-C content. A nutrient signaling response mediated by pyruvate induces Sirt1 protein in liver during fasting, where it interacts with and deacetylates PGC-1α in an NAD^+-dependent manner, increasing PGC-1α ability to coactivate HNF-4α and, therefore, upregulate gluconeogenic genes, but not mitochondrial genes (20). In addition, Sirt1-mediated deacetylation of FOXO1 has been shown to promote its transcriptional activity over gluconeogenic genes (39,40), suggesting an integrated regulation by insulin and Sirt1 over gluconeogenesis in treated animals. Moreover, Sirt1 transcription is inhibited by a NADH-mediated mechanism (41). In this context, Sirt1 seems to function as a nutrient sensor by decoding fluctuations in cellular NADH levels. Therefore, our observation of a substantial reduction of Sirt1 identifies this nutrient sensor as a potential mediator of the coordinated downregulation of gluconeogenesis. Recent data from Sun et al. (42) have shown that oral administration of resveratrol, an activator of Sirt1, improves glucose homeostasis and insulin sensitivity mainly though its ac-

tion on muscle. However, the potential for Sirt1 as a therapeutic target for diabetes in the liver is curtailed by its role in gluconeogenesis, as recently suggested by reduced HGO and improved glucose homeostasis and insulin sensitivity in *db/db* mice after hepatic Sirt1 silencing (43).

All in all, we present evidence to sustain that partial silencing of liver PEPCK-C in *db/db* mice leads to improved control of glycemia, insulinemia, and peripheral sensitivity to the hormone through its coordinate inhibition of key players responsible for the activation of liver gluconeogenesis, in the absence of a blockade at the level of mitochondria. In addition, we show that this model represents a departure from the view, recently challenged, that steatosis leads to insulin resistance. Finally, our observations join the growing body of evidence that indicates that PEPCK-C plays a key role in the control of hepatic energy metabolism in type 2 diabetes animals, validating liver PEPCK-C as a target for pharmaceutical intervention. Nonetheless, in view of the known discrepancy between the large contribution of gluconeogenesis to hepatic glucose production in small rodent models as compared to large animals (i.e., canine, human) the suitability of the approach should be further tested in a larger animal model.

REFERENCES

1. DeFronzo RA, Ferrannini E: Insulin resistance: a multifaceted syndrome responsible for NIDDM, obesity, hypertension, dyslipidemia, and atherosclerotic cardiovascular disease. *Diabetes Care* 14:173–194, 1991
2. Consoli A, Nurjhan N, Capani F, Gerich J: Predominant role of gluconeogenesis in increased hepatic glucose production in NIDDM. *Diabetes* 38:550–557, 1989
3. Hanson RW, Reshef L: Regulation of phosphoenolpyruvate carboxykinase (GTP) gene expression. *Annu Rev Biochem* 66:581–611, 1997
4. Sun Y, Liu S, Ferguson S, Wang L, Klepcyk P, Yun JS, Friedman JE: Phosphoenolpyruvate carboxykinase overexpression selectively attenuates insulin signaling and hepatic insulin sensitivity in transgenic mice. *J Biol Chem* 277:23301–23307, 2002
5. Valera A, Pujol A, Pelegrin M, Bosch F: Transgenic mice overexpressing phosphoenolpyruvate carboxykinase develop non-insulin-dependent diabetes mellitus. *Proc Natl Acad Sci U S A* 91:9151–9154, 1994
6. Burgess SC, Hausler N, Merritt M, Jeffrey FM, Storey C, Milde A, Koshy S, Lindner J, Magnuson MA, Malloy CR, Sherry AD: Impaired tricarboxylic acid cycle activity in mouse livers lacking cytosolic phosphoenolpyruvate carboxykinase. *J Biol Chem* 279:48941–48949, 2004
7. She P, Shiota M, Shelton KD, Chalkley R, Postic C, Magnuson MA: Phosphoenolpyruvate carboxykinase is necessary for the integration of hepatic energy metabolism. *Mol Cell Biol* 20:6508–6517, 2000
8. She P, Burgess SC, Shiota M, Flakoll P, Donahue EP, Malloy CR, Sherry AD, Magnuson MA: Mechanisms by which liver-specific PEPCK knockout mice preserve euglycemia during starvation. *Diabetes* 52:1649–1654, 2003
9. Hakimi P, Johnson MT, Yang J, Lepage DF, Conlon RA, Kalhan SC, Reshef L, Tilghman SM, Hanson RW: Phosphoenolpyruvate carboxykinase and the critical role of cataplerosis in the control of hepatic metabolism. *Nutr Metab* (*Lond*) 2:33, 2005

10. Cao H, van der Veer E, Ban MR, Hanley AJ, Zinman B, Harris SB, Young TK, Pickering JG, Hegele RA: Promoter polymorphism in PCK1 (phosphoenol-pyruvate carboxykinase gene) associated with type 2 diabetes mellitus. *J Clin Endocrinol Metab* 89:898–903, 2004

11. Landau BR, Wahren J, Chandramouli V, Schumann WC, Ekberg K, Kalhan SC: Contributions of gluconeogenesis to glucose production in the fasted state. *J Clin Invest* 98:378–385, 1996

12. Gomez-Valades AG, Vidal-Alabro A, Molas M, Boada J, Bermudez J, Bartrons R, Perales JC: Overcoming diabetes-induced hyperglycemia through inhibition of hepatic phosphoenolpyruvate carboxykinase (GTP) with RNAi. *Mol Ther* 13:401–410, 2006

13. Zeini M, Hortelano S, Traves PG, Gomez-Valades AG, Pujol A, Perales JC, Bartrons R, Bosca L: Assessment of a dual regulatory role for NO in liver regeneration after partial hepatectomy: protection against apoptosis and retardation of hepatocyte proliferation. *FASEB J* 19:995–997, 2005

14. Demoz A, Garras A, Asiedu DK, Netteland B, Berge RK: Rapid method for the separation and detection of tissue short-chain coenzyme A esters by reversed-phase high-performance liquid chromatography. *J Chromatogr B Biomed Appl* 667:148–152, 1995

15. Hrebicek J, Janout V, Malincikova J, Horakova D, Cizek L: Detection of insulin resistance by simple quantitative insulin sensitivity check index QUICKI for epidemiological assessment and prevention. *J Clin Endocrinol Metab* 87:144–147, 2002

16. Saha AK, Ruderman NB: Malonyl-CoA and AMP-activated protein kinase: an expanding partnership. *Mol Cell Biochem* 253:65–70, 2003

17. Samuel VT, Liu ZX, Wang A, Beddow SA, Geisler JG, Kahn M, Zhang XM, Monia BP, Bhanot S, Shulman GI: Inhibition of protein kinase C epsilon prevents hepatic insulin resistance in nonalcoholic fatty liver disease. *J Clin Invest* 117:739–745, 2007

18. Dhaunsi GS, Singh I, Orak JK, Singh AK: Antioxidant enzymes in ciprofi-brate-induced oxidative stress. *Carcinogenesis* 15:1923–1930, 1994

19. Hardie DG, Hawley SA, Scott JW: AMP-activated protein kinase: development of the energy sensor concept. *J Physiol* 574:7–15, 2006

20. Rodgers JT, Lerin C, Haas W, Gygi SP, Spiegelman BM, Puigserver P: Nutrient control of glucose homeostasis through a complex of PGC-1alpha and SIRT1. *Nature* 434:113–118, 2005

21. Ruijter JM, Gieling RG, Markman MM, Hagoort J, Lamers WH: Stereological measurement of porto-central gradients in gene expression in mouse liver. *Hepatology* 39:343–352, 2004

22. Zhao H, Yakar S, Gavrilova O, Sun H, Zhang Y, Kim H, Setser J, Jou W, LeRoith D: Phloridzin improves hyperglycemia but not hepatic insulin resistance in a transgenic mouse model of type 2 diabetes. *Diabetes* 53:2901–2909, 2004

23. Ono H, Katagiri H, Funaki M, Anai M, Inukai K, Fukushima Y, Sakoda H, Ogihara T, Onishi Y, Fujishiro M, Kikuchi M, Oka Y, Asano T: Regulation of phosphoinositide metabolism, Akt phosphorylation, and glucose transport by PTEN (phosphatase and tensin homolog deleted on chromosome 10) in 3T3–L1 adipocytes. *Mol Endocrinol* 15:1411–1422, 2001

24. Pocai A, Obici S, Schwartz GJ, Rossetti L: A brain-liver circuit regulates glucose homeostasis. *Cell Metab* 1:53–61, 2005

25. Uno K, Katagiri H, Yamada T, Ishigaki Y, Ogihara T, Imai J, Hasegawa Y, Gao J, Kaneko K, Iwasaki H, Ishihara H, Sasano H, Inukai K, Mizuguchi H, Asano T, Shiota M, Nakazato M, Oka Y: Neuronal pathway from the liver modulates energy expenditure and systemic insulin sensitivity. *Science* 312:1656–1659, 2006

26. Monetti M, Levin MC, Watt MJ, Sajan MP, Marmor S, Hubbard BK, Stevens RD, Bain JR, Newgard CB, Farese RV Sr, Hevener AL, Farese RV Jr: Dissociation of hepatic steatosis and insulin resistance in mice overexpressing DGAT in the liver. *Cell Metab* 6:69–78, 2007

27. Choi CS, Savage DB, Kulkarni A, Yu XX, Liu ZX, Morino K, Kim S, Distefano A, Samuel VT, Neschen S, Zhang D, Wang A, Zhang XM, Kahn M, Cline GW, Pandey SK, Geisler JG, Bhanot S, Monia BP, Shulman GI: Suppression of diacylglycerol acyltransferase-2 (DGAT2), but not DGAT1, with antisense oligonucleotides reverses diet-induced hepatic steatosis and insulin resistance. *J Biol Chem* 282:22678–22688, 2007

28. Kahn SE, Prigeon RL, Schwartz RS, Fujimoto WY, Knopp RH, Brunzell JD, Porte D Jr: Obesity, body fat distribution, insulin sensitivity and islet beta-cell function as explanations for metabolic diversity. *J Nutr* 131:354S–360S, 2001

29. Beale EG, Hammer RE, Antoine B, Forest C: Glyceroneogenesis comes of age. *FASEB J* 16:1695–1696, 2002

30. Kalhan SC, Mahajan S, Burkett E, Reshef L, Hanson RW: Glyceroneogenesis and the source of glycerol for hepatic triacylglycerol synthesis in humans. *J Biol Chem* 276:12928–12931, 2001

31. Drynan L, Quant PA, Zammit VA: Flux control exerted by mitochondrial outer membrane carnitine palmitoyltransferase over beta-oxidation, keto-genesis and tricarboxylic acid cycle activity in hepatocytes isolated from rats in different metabolic states. *Biochem J* 317:791–795, 1996

32. Drynan L, Quant PA, Zammit VA: The role of changes in the sensitivity of hepatic mitochondrial overt carnitine palmitoyltransferase in determining the onset of the ketosis of starvation in the rat. *Biochem J* 318:767–770, 1996

33. Hansmannel F, Mordier S, Iynedjian PB: Insulin induction of glucokinase and fatty acid synthase in hepatocytes: analysis of the roles of sterol-regulatory-element-binding protein-1c and liver X receptor. *Biochem J* 399:275–283, 2006

34. Gregori C, Guillet-Deniau I, Girard J, Decaux JF, Pichard AL: Insulin regulation of glucokinase gene expression: evidence against a role for sterol regulatory element binding protein 1 in primary hepatocytes. *FEBS Lett* 580:410–414, 2006

35. Mitro N, Mak PA, Vargas L, Godio C, Hampton E, Molteni V, Kreusch A, Saez E: The nuclear receptor LXR is a glucose sensor. *Nature* 445:219–223, 2007

36. Burgess SC, He T, Yan Z, Lindner J, Sherry AD, Malloy CR, Browning JD, Magnuson MA: Cytosolic phosphoenolpyruvate carboxykinase does not solely control the rate of hepatic gluconeogenesis in the intact mouse liver. *Cell Metab* 5:313–320, 2007

37. Tilghman SM, Belayew A: Transcriptional control of the murine albumin/alpha-fetoprotein locus during development. *Proc Natl Acad Sci U S A* 79:5254–5257, 1982

38. De Souza AT, Dai X, Spencer AG, Reppen T, Menzie A, Roesch PL, He Y, Caguyong MJ, Bloomer S, Herweijer H, Wolff JA, Hagstrom JE, Lewis DL, Linsley PS, Ulrich RG: Transcriptional and phenotypic comparisons of Ppara knockout and siRNA knockdown mice. *Nucleic Acid Res* 34:4486–4494, 2006

39. Nakae J, Cao Y, Daitoku H, Fukamizu A, Ogawa W, Yano Y, Hayashi Y: The LXXLL motif of murine forkhead transcription factor FoxO1 mediates Sirt1-dependent transcriptional activity. *J Clin Invest* 116:2473–2483, 2006

40. Frescas D, Valenti L, Accili D: Nuclear trapping of the forkhead transcription factor FoxO1 via Sirt-dependent deacetylation promotes expression of glucogenetic genes. *J Biol Chem* 280:20589–20595, 2005

41. Zhang Q, Wang SY, Fleuriel C, Leprince D, Rocheleau JV, Piston DW, Goodman RH: Metabolic regulation of SIRT1 transcription via a HIC1:CtBP corepressor complex. *Proc Natl Acad Sci U S A* 104:829–833, 2007

42. Sun C, Zhang F, Ge X, Yan T, Chen X, Shi X, Zhai Q: SIRT1 improves insulin sensitivity under insulin-resistant conditions by repressing PTP1B. *Cell Metab* 6:307–319, 2007

43. Rodgers JT, Puigserver P: Fasting-dependent glucose and lipid metabolic response through hepatic sirtuin 1. *Proc Natl Acad Sci U S A* 104:12861–12866, 2007

44. Kuznetsov AV, Strobl D, Ruttmann E, Konigsrainer A, Margreiter R, Gnaiger E: Evaluation of mitochondrial respiratory function in small biopsies of liver. *Anal Biochem* 305:186–194, 2002